Modeling the Target Acquisition Performance of Staring Array Imagers

March 1998

Richard Vollmerhausen and Ronald Driggers
Night Vision and Electronic Sensors Directorate
U.S. Army Communications and Electronics Command
Fort Belvoir, VA 22060

ABSTRACT

The sampling limitations associated with staring array imagers cause an aliased signal that corrupts the image. The aliased signal is a function of pre-sample blur, sampling frequency, and post-blur or image reconstruction. Papers in the literature have quantified aliasing and sample artifacts. However, the affect of these artifacts on target acquisition has not been quantified. That is, the relationship between the amount of aliasing or such display artifacts as visible raster and the target acquisition task performance of a human observer has not been established. In this paper, we provide a description of current efforts at the Night Vision and Electronic Sensors Directorate (NVESD) to quantify the relationship between the sampling artifacts generated by a sampled imager and target acquisition performance using that sensor.

Based on perception experiments performed at NVESD, the *MTF Squeeze* model was developed. The degraded performance due to under-sampling is modeled as an increase in system blur or, equivalently, a contraction or "squeeze" in the MTF. An improvement to the non-sampled linear systems performance model includes calculation of the sample-corrupted signal, calculation of the MTF squeeze, and the elimination of the half-sample rate spatial frequency limit. The *MTF Squeeze* technique is applied to two other sampling experiments and is shown to agree with their findings.

1.0 INTRODUCTION

The purpose of the investigation described in this paper is to provide a modification to the current linear systems sensor performance models to account for the artifacts caused by under-sampling. The sensor performance models that are available today, such as FLIR92 and Acquire, provide good results for those sensors that are adequately sampled. However, these current models are incorrectly applied to under-sampled sensors such as staring arrays. In the current models, under-sampling is characterized by a resolution limit equal to half the sample frequency. This approach is not consistent with sample theory, and the half sample cutoff can unfairly limit the predicted performance of staring imagers.

REPORT DOCUMENTATION PAGE

Form Approved OMB No. 0704-0188

1. REPORT DATE (DD-MM-YYYY)	2. REPORT TYPE	3. DATES COVERED (FROM - TO)
01-03-1998	Conference Proceedings	xx-xx-1998 to xx-xx-1998

4. TITLE AND SUBTITLE
Modeling the Target Acquisition Performance of Staring Array Imagers
Unclassified

5a. CONTRACT NUMBER
5b. GRANT NUMBER
5c. PROGRAM ELEMENT NUMBER

6. AUTHOR(S)
Vollmerhausen, Richard ;
Driggers, Ronald ;

5d. PROJECT NUMBER
5e. TASK NUMBER
5f. WORK UNIT NUMBER

7. PERFORMING ORGANIZATION NAME AND ADDRESS
Night Vision and Electronic Sensors Directorate
U.S. Army Communications and Electronics Command
Ft. Belvoir, VA22060

8. PERFORMING ORGANIZATION REPORT NUMBER

9. SPONSORING/MONITORING AGENCY NAME AND ADDRESS
Director, CECOM RDEC
Night Vision and Electronic Sensors Directorate, Security Team
10221 Burbeck Road
Ft. Belvoir, VA22060-5806

10. SPONSOR/MONITOR'S ACRONYM(S)
11. SPONSOR/MONITOR'S REPORT NUMBER(S)

12. DISTRIBUTION/AVAILABILITY STATEMENT
APUBLIC RELEASE
,

13. SUPPLEMENTARY NOTES
See Also ADM201041, 1998 IRIS Proceedings on CD-ROM.

14. ABSTRACT
The sampling limitations associated with staring array imagers cause an aliased signal that corrupts the image. The aliased signal is a function of pre-sample blur, sampling frequency, and post-blur or image reconstruction. Papers in the literature have quantified aliasing and sample artifacts. However, the affect of these artifacts on target acquisition has not been quantified. That is, the relationship between the amount of aliasing or such display artifacts as visible raster and the target acquisition task performance of a human observer has not been established. In this paper, we provide a description of current efforts at the Night Vision and Electronic Sensors Directorate (NVESD) to quantify the relationship between the sampling artifacts generated by a sampled imager and target acquisition performance using that sensor. Based on perception experiments performed at NVESD, the MTF Squeeze model was developed. The degraded performance due to under-sampling is modeled as an increase in system blur or, equivalently, a contraction or ?squeeze? in the MTF. An improvement to the non-sampled linear systems performance model includes calculation of the sample-corrupted signal, calculation of the MTF squeeze, and the elimination of the half-sample rate spatial frequency limit. The MTF Squeeze technique is applied to two other sampling experiments and is shown to agree with their findings.

15. SUBJECT TERMS

16. SECURITY CLASSIFICATION OF:			17. LIMITATION OF ABSTRACT	18. NUMBER OF PAGES	19. NAME OF RESPONSIBLE PERSON
a. REPORT	b. ABSTRACT	c. THIS PAGE	Public Release	14	Fenster, Lynn lfenster@dtic.mil
Unclassified	Unclassified	Unclassified			19b. TELEPHONE NUMBER International Area Code Area Code Telephone Number 703767-9007 DSN 427-9007

Before proceeding, the terms *aliasing* and *spurious response* are defined. It has become common practice among engineers to use the term *aliasing* to refer to any overlap between the sample-generated replica spectra and the baseband. In this paper, the word *aliasing* is only used in that context; that is, *aliasing* means that part of the replicated spectrum has overlapped, and therefore corrupted, the baseband spectrum. In this paper, the entire part of the image spectrum which results from sampling, other than the baseband, is referred to as *spurious response*. That is, in frequency space, *spurious response* is the Fourier transform of the sampling artifacts. Overlap between the spurious response and the baseband is called *aliasing*.

The spurious response of a sensor corresponds to artifacts in the sensor imagery; it is a much better indicator of sampling efficacy than the half sample rate. The spurious response of a sensor can be described in a manner very similar to the sensor Modulation Transfer Function (MTF). The greatest barrier in the use of spurious response to characterize sensor performance is the calibration of human reaction to spurious response.

NVESD has recently completed a set of character recognition experiments. The results of these experiments provide a relationship between the performance degradation due to spurious response and the degradation associated with an additional blur. This relationship is used to modify the MTF of the sensor in a way that degrades predicted performance by an amount necessary to account for the observer reaction to the spurious response of the sensor. The modified MTF is used in the existing sensor models to quantify the impact of under-sampling on sensor performance.

This paper first describes the background of staring array sensor modeling including the history of the spurious response approach. The calculation of spurious response in a sampled imaging system is then presented. An MTF modification is then implemented based in the NVESD character recognition experiment and shown to give accurate predictions of sensor/human performance as a function of spurious response. The procedure for implementing model modifications is provided. Finally, the model modification is applied to two previous sampling experiments and is shown to accurately characterize the results of those experiments.

In this investigation, we assume that the sensor is stationary with respect to the scene. The spurious responses discussed in this report are, indeed, present when there is relative scene to sensor motion; however, the spatial sampling rate changes when the sensor is panned across the scene. The investigation given here applies only to *static* performance.

2.0 BACKGROUND

This decade has seen significant advances in the development of infrared staring arrays. Staring arrays have substantially increased sensitivity over existing scanned systems since longer integration times can be realized. However, the limitations on detector spacing and fill factors can result in resolution characteristics very different from scanning systems. There is a large literature base on the characterization of the under-sampled effects of staring arrays, and we present an overview in this section. This overview is presented in three parts: performance measurements of sensors, theory of under-sampled systems, and experimentation to characterize under-sampled systems.

Minimum Resolvable Temperature Difference (MRTD or just MRT) is the primary measure of imaging infrared sensor performance.[1] A number of artifacts are seen when measuring the MRT of staring imagers; for example, the MRT extends beyond the half sample rate of the sensor.[2, 3] Other artifacts include the increase in MRT measured values for spatial frequencies between 0.6 to 0.9 times the half-sample rate of the sensor.[4] Laboratory measurements of these sampled system artifacts have been explained.[5] However, it is not clear how these artifacts affect field performance. Phasing, or the relative lateral position between the staring array and a scene, is more important in staring arrays than with scanning systems. Artifacts include edge and position uncertainties associated with the phase. The performance of sensor systems that are under-sampled is a strong function of phase, especially during the imaging of laboratory bar pattern targets.

In the past, laboratory measurements have been used to provide useful prediction of field performance. The relationship between laboratory measurements and field performance has been an overall success. This does not appear to be the case with staring arrays, as the relationship between laboratory measurement and field performance has large discrepancies that have not been characterized. While laboratory measurements of staring arrays are available, there is limited field performance data on these same systems. The little data that is available does not appear to have the same laboratory to field relationship seen with first generation and second generation sensors.[6] That is, the discrepancy between laboratory performance and field performance is increased for staring arrays.

There are a number of theories on how the presence of spurious response affects human performance. One such theory is to treat spurious response as fixed pattern noise[7]. Other approaches to performance characterization of under-sampled imagery included the use of an eye model calibrated on non-aliased imagery and then applied to aliased imagery to determine the eye response.[8] While this technique showed that aliasing reduces the probability of finding targets, no general relationship was developed that describes the effects of aliasing and spurious response. The study did, however, show a general trend that an increase in the amount of aliasing corresponds to a decrease in probability of detection. There have been additional studies that have suggested a change in the Johnson cycle criteria can compensate for the differences in staring and scanning sensor performance.[9] It was shown by an experiment, however, that there was a greater difference between the staring sensors than between the staring and scanning sensors. Sampled imagery has even been described using information density and efficiency, but it has not been calibrated for human responses.[10] This is also the case for the ATR response to sampled imagery where a general relationship is not available, but a trend has been demonstrated.[11]

There are a number of experiments that were intended to investigate the effects of under-sampling. These experiments accomplished their objective of demonstrating that there is a strong relationship between a reduction in recognition performance with under-sampling. One such experiment was specifically designed to demonstrate reductions in the recognition of vehicle images that had been under-sampled.[17] This particular experiment studied the reduction in recognition rate as a function of samples per detector angular subtense (or detector dwell). The investigation found that the two-dimensional sample density (as well as detector dwell) is a critical performance parameter. A second experiment supports the results described above; in this experiment, identification was studied as a function of samples per detector dwell.[18] These results also showed that both sampling aperture and sample spacing are critical factors in human performance. The authors used these two experiments to determine whether a model modification could be developed based on the concept of samples per dwell. There appeared to be no direct functional relationship between samples per detector dwell and the reduction in human recognition performance that could be integrated into existing models.

Overall, the literature supports the use of aliasing and spurious response calculations to characterize under-sampled systems.[12,13,14,15] The shortfall here is the calibration of human observation to spurious response, hence, the character experiment described in this report. The character experiment was used to establish a relationship between spurious response and human recognition performance. This new approach to predicting performance degradation due to sampling was incorporated into the NVESD performance models. The data from the experiments described in References 17 and 18 was used to validate the new approach.

3.0 CALCULATING SPURIOUS RESPONSE

The amount of spurious response in an image is dependent on the spatial frequencies that comprise the scene and on the pre-blur, sampling, and post-blur characteristics of the sensor. However, the spurious response *capacity* of an imager can be determined by characterizing the imager response to a point source. This characterization is identical to the Modulation Transfer Function (MTF) approach for continuous systems.

The response function $R_{sp}(\omega)$ for a sampled imager is found by examining the impulse response of the system.[13,14,15] This procedure is identical to that used with non-sampled systems. The function being sampled is h(x), the point spread function of the pre-sampled image. Assume the following definitions:

$$\upsilon = the\,sample\,frequency\,in\,radians$$
$$\omega = frequency\,in\,radians$$
$$d = spatial\,offset\,of\,origin\,from\,a\,sample\,point$$
$$H(\omega) = Pre-sample\,MTF\,(optics\,and\,detector)$$
$$P_{ix}(\omega) = Display\,MTF\,(CRT\,spot, electronic\,sample\,and\,hold)$$

Then the response function $R_{sp}(\omega)$ is given by the following equation.

$$R_{sp}(\omega) = \sum_{n=-\infty}^{n=\infty} H(\omega - n\upsilon)\, e^{-i(\omega - n\upsilon)d}\, P_{ix}(\omega) \qquad (1)$$

$$R_{sp}(\omega) = H(\omega) e^{-i\omega d}\, P_{ix}(\omega) + \sum_{all\ n \neq 0} H(\omega - n\upsilon)\, e^{-i(\omega - n\upsilon)d}\, P_{ix}(\omega)$$

The response function has two parts, a transfer term and spurious response terms. The n=0 term in Equation 1 is the transfer response (or baseband response) of the imager. The transfer response does not depend on sample spacing, and it is the only term that remains for very small sample spacing. A sampled imager has the same transfer function as a non-sampled (that is, a very well sampled) imager.

However, a sampled imager always has the additional response terms (the $n \neq 0$ terms), which will be referred to as *spurious response*. The spurious response terms in Equation 1 are filtered by the display MTF, $P_{ix}(\omega)$, in the same way that the transfer response is filtered. However, the position of the spurious response terms on the frequency axis depends on the sample spacing. Also, the phase relationship between the transfer response and the spurious response depends on the sample phase. See Figure 1 for a graphical illustration of the transfer and spurious response terms.

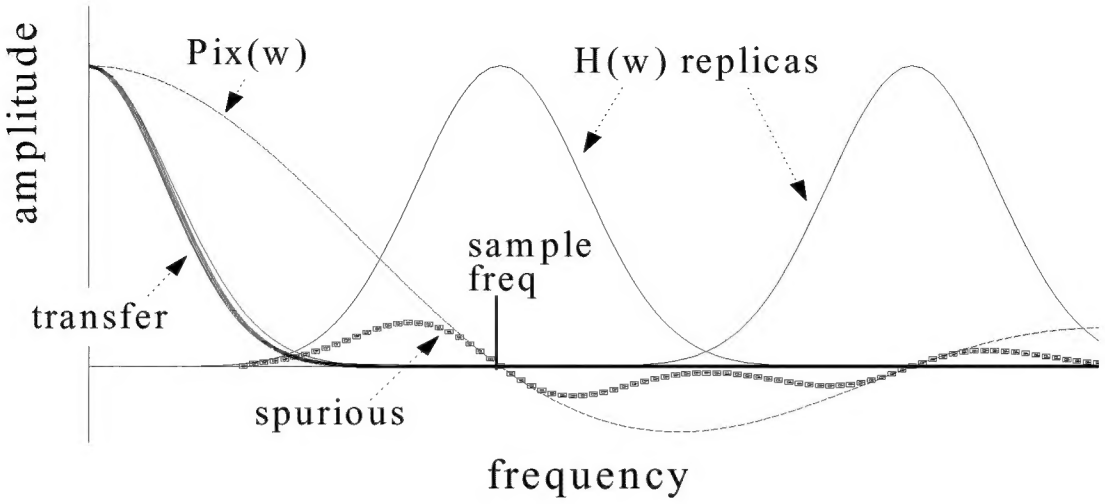

Figure 1. Notional plot of the sampled imager response function. The pre-sample MTF H(ω) is replicated at the sample frequency. The display and eye MTF $P_{ix}(\omega)$ filter both the baseband signal and the replicated signal. The transfer response is the pre-sample MTF multiplied by the display and eye MTF. The pre-sample replicas are also filtered by the display and eye MTF and become the spurious response.

It was found during the character experiment that performance could be related to the ratio (SR) of integrated spurious response to baseband response. See Equation 2 below. If the various replicas of the pre-sample blur overlap, then the signals in the overlapped region are root-sum-squared.

$$SR_{\varepsilon} = \frac{\int_{-\infty}^{\infty} (Spurious\ response)\, d\varepsilon}{\int_{-\infty}^{\infty} (Baseband\ \ signal)\, d\varepsilon} \qquad (2)$$

4.0 EQUIVALENT BLUR EXPERIMENT

A character recognition experiment was conducted at NVESD in order to investigate human recognition characteristics as a function of spurious response. The results of the experiment have provided a means for quantifying performance degradation due to spurious response as a relative increase in sensor blur. The experiment involved the recognition of 3500 character pairs that had been processed with various pre-sample blurs, sample spacings, and display characteristics. The test subjects were 19 Army Sergeants and 1 civilian.

Six characters were used in the experiments: 2, 3, 5, 8, 9, and E. Examples of the numerals 2 and 3 are shown in Figure 2. These characters were shown to be equally recognizable at the limits of human perception by the University of Rochester.[16] Two characters were presented in each image, and both had to be recognized correctly to score a correct call.

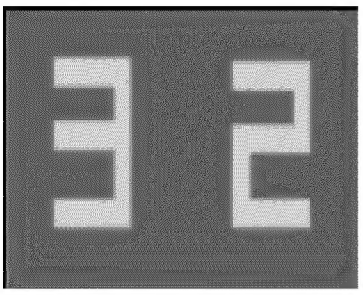

Figure 2. Two examples of the University of Rochester letters used for the experiment.

There were seven experiments involving 20 cases (20 combinations of blur and spurious response) with each case consisting of 25 character pairs. The pre-blur was always Gaussian. Post-blur was both Gaussian and Rect function; two display blurs were used in order to represent a range of display options from CRT to flat panel. Baselines were taken for each blur combination without spurious response. Experiments were then run with the same blurs but with various, controlled amounts of spurious response added by varying the sample spacing.

The display reconstruction blur was always very large (corresponding to an small transfer function) compared to the monitor transfer function and the transfer function of the eye, so these responses were neglected in the spurious response calculation. The letters were presented with 256 gray levels and a 0 gray level background. The observers were allowed to adjust the gain and contrast of the monitor to their liking. The experiments comprised both one dimensional and two dimensional spurious responses.

In the following analysis, blur dimension is in character units and is defined by the 4.3% amplitude. Each character was 46 units high and 36 units wide.

For the baseline cases without spurious response, the probability of recognition versus blur is shown in Figure 3. This figure shows probability of recognition versus blur radius when no spurious response was present. Blur in both horizontal and vertical are equal. The asterisks show results for the rect display and the "hour glass" symbols show the Gaussian results.

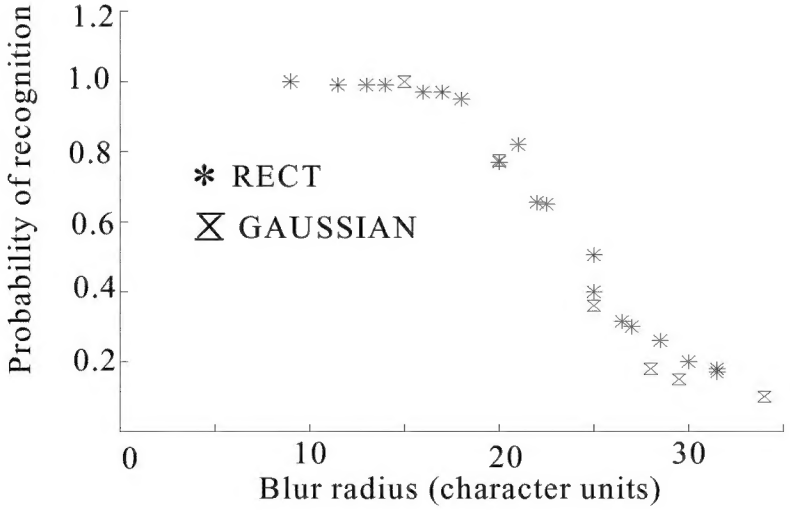

Figure 3. Probability of character recognition versus blur radius.

For each spurious response case, we found the baseline case without spurious response which gave the same probability of recognition. We then developed an equation which related the actual blur (with spurious response) to the increased baseline blur (without spurious response) which gave the same probability. The increase in blur for both the two dimensional spurious response case and the one dimensional spurious response case was fit by using only simple equations.

The results for the two dimensional case (same spurious response both horizontally and vertically) is shown in Figure 4. The two dimensional relative blur increase fit shown is

$$RI = \frac{1}{1 - 0.32SR} \tag{3}$$

where SR is the spurious response ratio of the sensor defined by Equation 2.

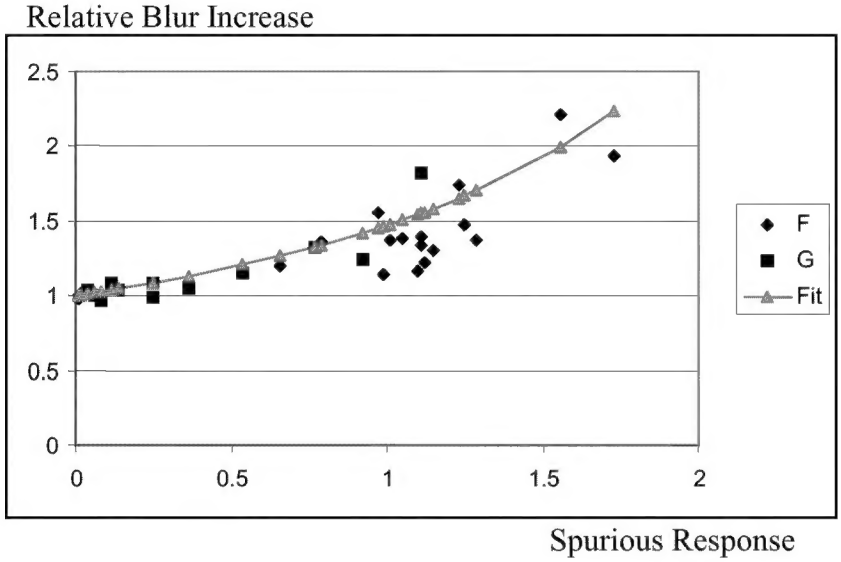

Figure 4. Plot of spurious response (in both dimensions) versus the relative blur increase required to give same probability without spurious response. "F" is Rect function display (flat panel), "G" is Gaussian display, and "Fit" is the curve fit.

The one dimensional spurious response fit, along with the one dimensional data, is shown in figure 5. The relative blur increase (RI) is

$$RI = \frac{1}{\sqrt{1 - 0.32SR}} \tag{4}$$

Spurious response (and sampling effects) applied only in one dimension clearly has less of an effect on the human recognition process than spurious responses in both directions. In fact, it is fortunate that the increase in blur follows a separable function in x and y relative to the two-dimensional response, as this is typically an assumption in current sensor models such as the NVESD FLIR92 sensor performance model.

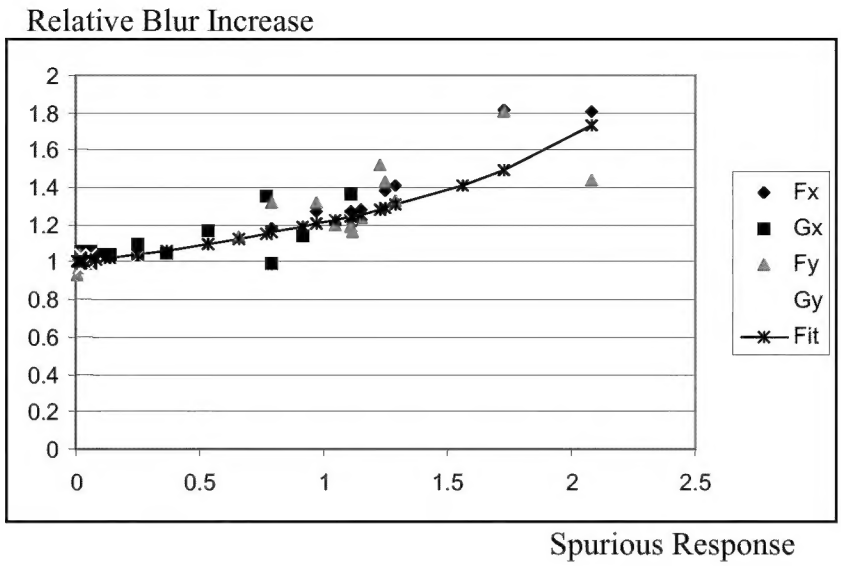

Figure 5. Plot of spurious response in one dimension versus the relative blur increase required to give same probability without spurious response.

We emphasize that, for both Equations 3 and 4, *the relative increase in blur is in two dimensions.* That is, even if the spurious response is in one direction, the relative increase shown in Equation 4 is applied to both directions. The authors intuitively suspect that the blur increase defined by Equation 3 can be applied to the MTF in one direction based on the spurious response in that direction. That is, rather than applying Equation 4 to both directions, Equation 3 would be applied to one direction. However, this was not demonstrated in the current experiment.

5.0 MTF SQUEEZE

By the Similarity Theorem (sometimes called the scaling property of Fourier Transforms), a proportional increase in the spatial domain is a contraction in the frequency domain. This turns an equivalent blur increase into an MTF contraction, and makes the equivalent blur technique easy to apply to the NVESD performance models.

We can use the Similarity Theorem to apply the spurious response correction in the frequency domain. Instead of an increase in the effective size of the point spread function, we contract the Modulation Transfer Function. The contraction as a function of spurious response which is equal in two dimensions is:

$$Contraction = 1.0 - 0.32\,SR \qquad (5)$$

For spurious response in one dimension, the MTF contraction is:

$$Contraction = \sqrt{1.0 - 0.32\,SR} \qquad (6)$$

Figure 6 illustrates the application of contraction to the system MTF in the thermal MRTD model. The spurious response is calculated independently in the horizontal and vertical directions. At each (frequency, amplitude) point, the frequency is scaled by the contraction factor shown in Equation 5. The contraction is applied in each direction separately depending on the spurious response in that direction. The contraction is applied to the signal MTF but not to the noise MTF. The reason for using the Equation 5 contraction factor, rather than the Equation 6 factor, is described below.

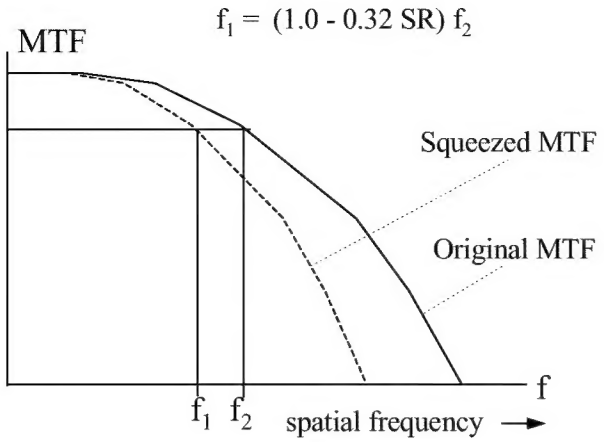

Figure 6. Application of the MTF Squeeze. Contraction shown is applied independently to the horizontal and vertical MTFs depending on the spurious response in each direction. Contraction is applied to signal MTF, not the noise MTF. Note that the contraction factor from Equation 5 is used, not the factor in Equation 6; the reason is described in the text.

In the most recent NVESD performance models, a single 2D MRTD is generated by combining the horizontal and vertical MRTDs. This procedure is illustrated in Figure 7. The horizontal and vertical frequencies achieved at each temperature are geometrically averaged. In the Acquire model, the 2D MRTD is used with the square root of the target area, the target range, and the target thermal contrast to establish the number of resolvable cycles across the target. Given a number of resolvable cycles across the target, the Johnson criteria is used to predict the probability of detecting, recognizing, or identifying the target.

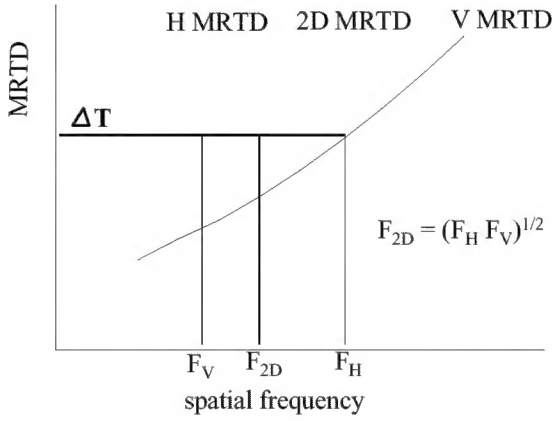

Figure 7. Generating 2D MRTD from the Horizontal (H MRTD) and Vertical (V MRTD)

The use of geometrically averaged horizontal and vertical MTRD for range prediction makes sense. If, for example, the MTRD frequencies are doubled in both axes for each temperature contrast, and the noise is in some way appropriately scaled, then the sensor to target range will double, not quadruple. This is a reasonable result, because it indicates equivalent performance for equivalent images.

The current FLIR92 and Acquire models do not treat the horizontal and vertical axes independently when estimating range performance; in essence, an equivalent blur is calculated and used to predict range. The MTF Squeeze developed using symetrical blurs is therefore easy to apply to the current models. Consider the two dimensional frequency

$$\rho_{2d} = \sqrt{\xi\eta} \qquad \text{[cycles per milliradian]} \tag{7}$$

where ξ and η are the horizontal and vertical spatial frequencies. To determine the transfer "squeeze" effect in terms of a two dimensional blur, we let the overall squeeze effect follow the guidelines

$$(1-0.32SR)\rho_{2d} = (1-0.32SR)\sqrt{\xi\eta} \tag{8}$$

If we now apportion the weighting in each of the directions, then

$$(1-0.32SR)\sqrt{\xi\eta} = \sqrt{(1-0.32SR)\xi(1-0.32SR)\eta} \tag{9}$$

so that the squeeze in any one of the directions is modeled in the same manner as that of the two-dimensional squeeze. That is, the squeeze in the horizontal transfer function can be modeled by $1-0.32SR_x$ where SR_x is the spurious response in the horizontal direction. The vertical squeeze is modeled by the same squeeze factor equation but using SR_y.

6.0 VALIDATION

The technique described in this paper was applied to experimental data gathered in two previous sampling experiments at NVESD. Both of the previous eeriments used tactical military vehicles in the image sets.

The first experiment was performed by J. D'Agostino, M. Friedman, R. LaFollette, and M. Crenshaw and described in "An Experimental Study of the Effects of Sampling on FLIR Performance."[17] In this experiment, a rectangular blur (corresponding to detector IFOV with no optical degradation) was applied to imagery. Three different IFOVs (50 microradians, 100 microradians, and 200 microradians) were sampled with different spacings (50 microradians, 100 microradians, and 200 microradians). The display of the imagery was kept at the same magnification, so a single 50 microradian sample corresponded to a display sample. Bilinear interpolation was taken for the 100 microradian samples and double bilinear interpolation was taken for the 200 microradian samples. The display was a CRT with a height of 15.24 centimeters, and a viewing distance of around 30 centimeters was assumed (this drives the display spot size). The display was assumed to have a luminance of 10 milliLamberts. The display also had a sample-and-hold that was modeled in the horizontal MTF.

The spurious response was calculated for each of the cases. The MTF cutoff was also determined for the baseband, where the cutoff frequency (in cycles per milliradian) was taken at 10 percent of full modulation. The MTF included the detector shape, the bilinear interpolation, the sample and hold, the display spot, and the eye. For each case, the probability of recognition was reported in Reference 17.

During the experiment, a baseline was not collected of the probability of recognition without spurious response for each different blur. We established a baseline using the TTPF equation and the four probabilities with the least amount of spurious response. The baseline calibration determined an N_{50} corresponding to 2.7 cycles per milliradian. Note, again, that these calibration points were those with the least amount of spurious response (Blocks 1, 2, 3, and 6).

Using the TTPF baseline to make an estimate for probability of recognition as a function of MTF cutoff (not spurious response corrected), the measured probability of recognition and TTPF baseline probability estimates are shown in Figure 8.

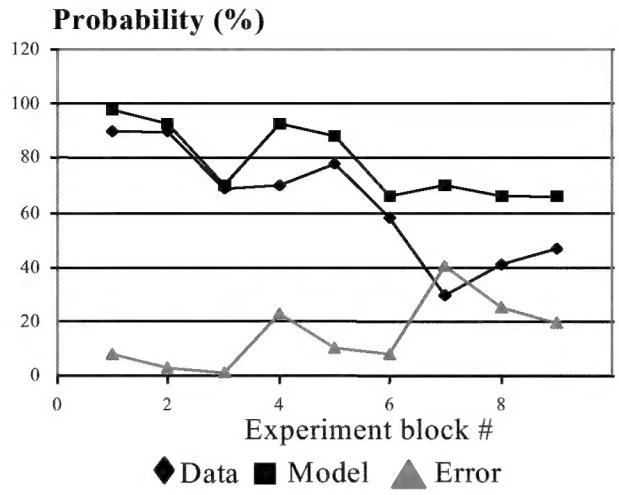

Figure 8. TTPF predicted baseline probabilities versus measured probabilities.

The TTPF was again applied to estimate the probability of recognition for each block; however, this time the MTF cutoff was corrected for spurious response using the spurious response "squeeze" factor. The results of the probability of recognition estimates are shown in Figure 9. Note that those blocks that corresponded to the largest spurious response went from large errors to significantly smaller errors.

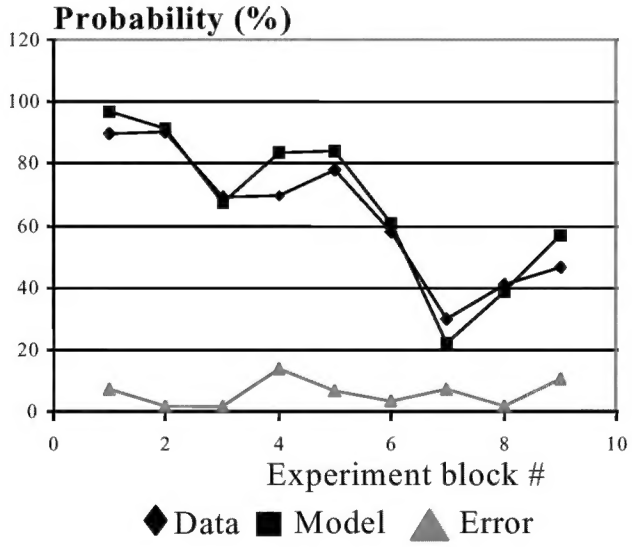

Figure 9. TTPF baseline with SR Correction versus measured probabilities.

A second experiment was also investigated with the new MTF Squeeze approach in order to further validate the concept.[18] "Thermal Model Improvement Through Perception Testing," by James Howe, Luke Scott, Scott Pletz, John Horger, and Jonathan Mark was analyzed for spurious response within the data. In the referenced effort, an intentional undersampling experiment was conducted, where the horizontal sample rate, vertical sample rate, and vertical detector size was varied in order to evaluate the effects of undersampling.

In this experiment, pre-sample blur included an optical blur, a detector shape blur, and a detector sample-and-hold (in the horizontal direction). The sample spacing was given as 1, 1.5, and 2 samples per detector IFOV and was applied the same in the horizontal and vertical direction (note that the sample spacing changes in the vertical direction since the IFOV changes in the vertical direction) The reconstruction blur included bi-linear interpolation, a CRT spot, horizontal sample-and-hold, and the human eye. The MTF was calculated in both directions and the spurious response was determined.

The five data points with the least amount of spurious response were used to calibrate the TTPF curve. The 50% probability of recognition occurred at 3.15 cycles per milliradian. Using the calibrated TTPF curve, the Howe data was plotted in a maner that was uncorrected for spurious response (the cutoff frequencies in the horizontal and vertical directions were combined directly as the geometric mean). The probability of recognition was then plotted as a function of spatial frequency as shown in Figure 10. The Howe data was then corrected by a squeeze in the frequency associated with each probability measurement. The squeeze was a function of spurious response. The results were again plotted as a function of spatial frequency as shown in Figure 11. The MTF Squeeze correction brought the predicted and measured probabilities into close agreement.

We have shown two cases where application of the squeeze technique has resulted in good correspondence between measured and predicted data. It appears that the squeeze approach is a reasonable one that can accurately characterize the performance impact of undersampling in terms of an equivalent MTF reduction.

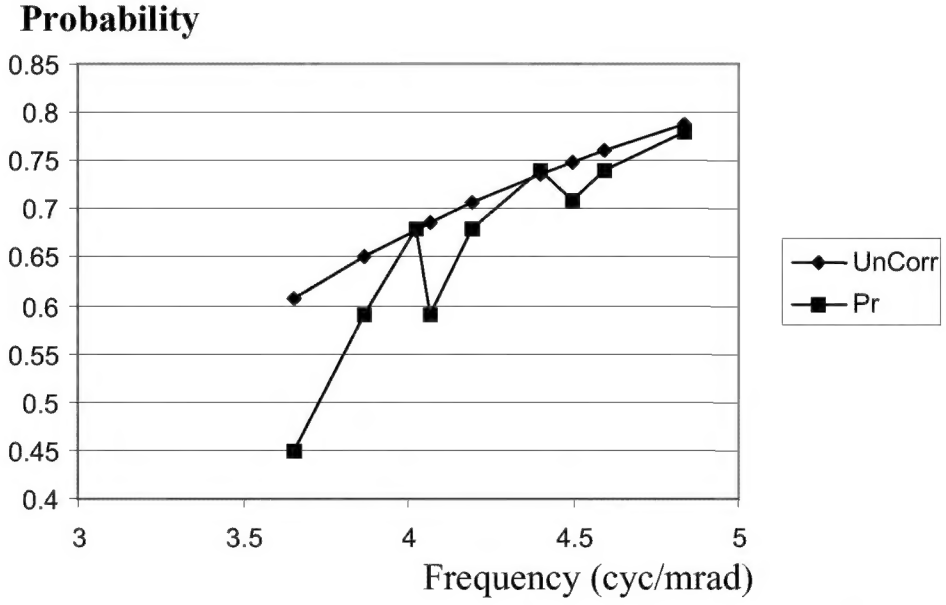

Figure 10. TTPF predicted baseline probabilities versus measured probabilities.

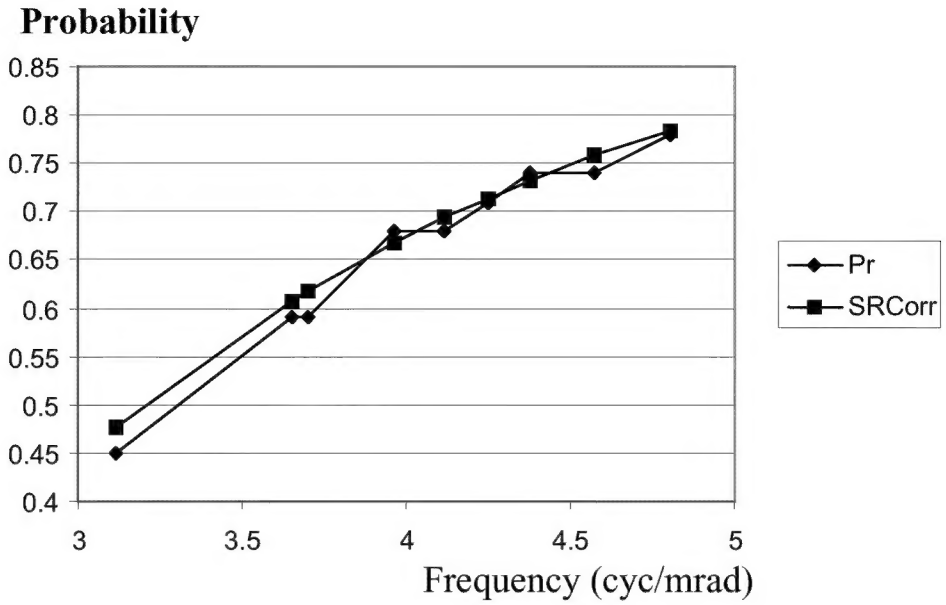

Figure 11. Corrected Howe Results

7.0 CONCLUSION

We provided a description of the spurious response of a sampled imager and provided the equations needed to calculate the spurious response in performance models. The results of a character recognition experiment were described which allowed the performance degradation due to spurious reponse to be equated to an effective increase in system blur. An equation was developed that quantified the amount of MTF squeeze or contraction to apply to the system MTF in order to account for the performance degradation caused by the spurious response. The MTF Squeeze technique was applied to two previous sampling experiments conducted at NVESD. The D'Agostino et. al. experiment and the Howe et. al. experiment were accurately characterized using the spurious response and MTF squeeze approach. This implementation is currently being evaluated by NVESD, and preliminary results show promise as an adaptation for undersampled systems.

8.0 REFERENCES

1. J. M. Lloyd, *Thermal Imaging Systems*, Plenum Press, New York, 1975, pp 184
2. G. Holst, "Effects of Phasing on MRT Target Visibility," *SPIE Vol 1488, Infrared Imaging Systems: Design, Analysis, Modeling, and Testing II,* March, pg 90, 1991.
3. C. M. Webb, "Results of Laboratory Evaluation of Staring Arrays," *SPIE Vol 1309, Infrared Imaging Systems: Design, Analysis, Modeling, and Testing,* pg. 271, 1990.
4. C. M. Webb, "Dynamic Minimum Resolvable Temperature Difference for Staring Focal Plane Arrays," *Proceedings of the IRIS Speciality Group on Passive Sensors,* Infrared Information Analysis Center, ERIM, Ann Arbor, MI, 1993.
5. R. Vollmerhausen, R. Driggers, C. Webb and T. Edwards, "Staring Imager Minimum Resolvable Temperature (MRT) Measurements Beyond The Sensor Half Sample Rate," accepted by *Optical Engineering*, Jan, 1998.

6. W. Wittenstein, W. Fick, and U. Raidt, "Range Performance of Two Staring Imagers - Presentation of the Field Trial and Data Analysis," *SPIE Vol 2743*, Page 132.

7. S. Park and R. Hazra, "Aliasing as Noise: A Quantitative and Qualitative Assessment," *SPIE Vol 1969*, Pg 54.

8. T. Meitzler and G. Gerhart, "Spatial Aliasing Effects in Ground Vehicle IR Imagery," *SPIE Vol 1689,* Pg 226.

9. P. Owen and J. Dawson, "Resolving The Differences In Oversampled and Undersampled Imaging Sensors: Updated Target Acquistion Modeling Strategies for Staring and Scanning FLIR Systems," *SPIE Vol 1689,* 1992, pg 251.

10. F. Huck, S. Park, D. Speray, and N. Halyo, "Information Density and Efficiency of Two-Dimensional Sampled Imagery, *SPIE Vol 310,* 1981, Pg 36.

11. J. Kruthers, T. Williams, G. O'Brien, K. Le, and J. Howe, "A Study of the Effects of Focal Plane Array Design Parameters on ATR Performance," *SPIE Vol 1957*, pg 165.

12. S. Park and R. Schowengerdt, "Image Sampling, Reconstruction, and the Effect of Sample-Scene Phasing," *Applied Optics*, Vol 21, No 17, pg 3142.

13. W. Wittenstein, J. Fontanella, A. Newberry, and J. Baars, "The Definition and the OTF and the Measurement of Aliasing for Sampled Imaging Systems," *Optica Acta*, Vol 29, No 1, pg 50.

14. R. Vollmerhausen, "Impact of display modulation transfer function on the quality of sampled imagery," *Aerospace/Defense Sensing and Controls.* Society of Photo-Optic and Instrumentation Engineers, paper 2743-09, 1996.

15. R. Vollmerhausen, "Display of Sampled Imagery," *IRIA-IRIS Proceedings: Meeting of the IRIS Specialty Group on Passive Sensors,* Vol. 1, pp 175-192, 1990.

16. *Instructions for the Use of the RIT Alphanumeric Resolution Test Object,* Graphic Arts Research Center, Institude of Technology, Rochester, New York.

17. J. D'Agostino, M. Friedman, R. LaFollette, and M. Crenshaw, "An Experimental Study of the Effects of Sampling on FLIR Performance," *Proceedings of the IRIS Speciality Group on Passive Sensors,* Infrared Information Analysis Center, ERIM, Ann Arbor, MI, 1990.

18. J. Howe, L. Scott, S. Pletz, J. Horger, and J. Mark, "Thermal Model Improvement Through Perception Testing," *Proceedings of the IRIS Speciality Group on Passive Sensors,* Infrared Information Analysis Center, ERIM, Ann Arbor, MI, 1989.